The CP43 Core Antenna Complex of Photosystem II Possesses Two Quasi-Degenerate and Weakly Coupled Qy-Trap States

ARTICLE *in* THE JOURNAL OF PHYSICAL CHEMISTRY B · DECEMBER 2000

Impact Factor: 3.3 · DOI: 10.1021/jp0025431

8 AUTHORS, INCLUDING:

Ryszard Jankowiak
Kansas State University
193 PUBLICATIONS **4,702** CITATIONS

SEE PROFILE

Valter Zazubovich
Concordia University Montreal
43 PUBLICATIONS **711** CITATIONS

SEE PROFILE

The CP43 Core Antenna Complex of Photosystem II Possesses Two Quasi-Degenerate and Weakly Coupled Q_y-Trap States

R. Jankowiak,*,† V. Zazubovich,† M. Rätsep,† S. Matsuzaki,† M. Alfonso,‡ R. Picorel,‡,§ M. Seibert,§ and G. J. Small*,†

Ames Laboratory-USDOE and Department of Chemistry, Iowa State University, Ames, Iowa 50011, E. E. Aula Dei, CSIC, 50080-Zaragoza, Spain, and National Renewable Energy Laboratory, 1617 Cole Boulevard, Golden, Colorado 80401

Received: July 18, 2000; In Final Form: September 13, 2000

The CP43 chlorophyll *a*-core protein complex plays an important role in funneling excitation energy absorbed by more peripheral antenna complexes of photosystem II (PSII) to the reaction center (RC). Identification and characterization of the lowest energy Q_y-states of CP43 is important for understanding the kinetics of excitation energy transfer (EET) from CP43 to the RC. We report the results of several types of spectroscopic experiments performed at liquid He temperatures on the isolated CP43 complex from spinach. Nonphotochemical hole burning (NPHB) and triplet bottleneck hole burning spectroscopies as well as zero-phonon hole (ZPH) action and Stark hole burning spectroscopies were employed. Two quasi-degenerate trap states at 682.9 nm (B state) and 683.3 nm (A state) are identified. The widths of their mainly inhomogeneously broadened Q_y-absorption bands are 45 and 120 cm^{-1}, respectively. The uncorrelated site excitation distribution functions (SDF) of the two states are nearly the same as their absorption bands since the electron−phonon coupling is weak (optical reorganization energies of $\sim$6 cm^{-1}). The NPHB spectra establish that the B state is the primary trap for EET from higher energy Q_y-states. The permanent dipole moment change ($\Delta\mu$) of the $S_0 \rightarrow Q_y$ transition for both the B and A states is small, $f\cdot\Delta\mu = 0.25 \pm 0.05$ and 0.47 ± 0.05, respectively, where f is the local field correction factor. These values, together with the weak electron−phonon coupling and other results, indicate that both states are highly localized on a single Chl *a* molecule. Holewidth measurements led to the remarkable finding that the rates of A → B and B → A EET processes are extremely slow, $\sim$(6 ns)$^{-1}$. This suggests that the Chl *a* molecules of the two states belong to different layers of Chl *a* molecules located at opposite sides of the membrane. The intriguing question of why CP43 possesses two quasi-degenerate trap states that are so weakly coupled is addressed. The possibility that they play a role in the photoinhibitory and photoregulatory processes is raised.

1. Introduction

The CP43 and CP47 protein−chlorophyll *a* (Chl *a*) complexes constitute the core antenna of photosystem II (PSII). They are present in all oxygenic photosynthetic organisms in a constant ratio of 1:1 with respect to the D1−D2 reaction center (RC) complex. The assembly of these three complexes along with the peripheral Chl *a*/*b* light-harvesting complex II (LHC II) and the minor Chl *a*/*b* complexes (CP24, CP26, and CP29) and the extrinsic proteins compose the O_2-evolving PSII.[1]

Given that CP43 and CP47 are proximal to the RC it is generally held that they serve, in part, to funnel energy absorbed by LHC II and the minor antenna complexes to the RC. CP43 and CP47 are sequence related and both possess three pairs of transmembrane α-helices.[1,2] Thus, one expects that CP43 and CP47 should contain about the same number of Chl *a* molecules. Prior to 1992, values for the CP43 Chl *a* content of 4−7,[4,5] 10−25,[6] 11[7], and 9[8] were reported. Values of 18−20,[9] 12−15,[10] and 14[11] were subsequently reported. Recently, the structure of CP47−RC was investigated by electron crystallography of two-dimensional crystals.[2,3] It led to the preliminary location of 14 Chl *a* molecules in CP47. Thus, the Chl *a* content of CP43 is most likely also close to 14. The structure indicates that the 14 Chl *a* molecules occur in two layers near the luminal and stroma sides of the membrane. It is likely that this motif exists for CP43. Electron microscopy and image averaging techniques applied to isolated and purified PSII particles have recently provided valuable information on how the antenna proteins are arranged.[12−14] CP43, which is closely associated with the D1 polypeptide, appears to be in a position favorable for accepting excitation energy from CP26 and funneling that energy to the RC. Its location is more peripheral than that of CP47 which appears to play a role in the dimerization of the PSII core complex. Thus, the role of CP43 in transferring energy from the peripheral complexes to the RC may be more important than that of CP47. Interestingly, CP43 is very sensitive to conditions under which PSII is photoinhibited.[15,16] This may correlate with the close proximity of CP43 to the D1 RC polypeptide which is known to be the main target of the photoinhibition process. It might also be involved in the regulatory pathway that controls the amount of excitation energy reaching the RC and, thus, protecting it against photoinhibitory damage.

* Corresponding authors. E-mail: gsmall@ameslab.gov; jankowiak@ameslab.gov.
† Ames Laboratory.
‡ E. E. Aula Dei.
§ National Renewable Energy Laboratory.

10.1021/jp0025431 CCC: $19.00
Published on Web 11/16/2000

Presented here are the results of spectral hole burning experiments performed at liquid helium temperatures that were mainly designed to identify and characterize the two lowest energy Q_y-states of CP43 and to determine the kinetics of excitation energy transfer (EET) between them. Low-temperature absorption spectra obtained several years ago[17−20] established that the CP43 complex exhibits a lowest energy absorption band or shoulder at 682−683 nm and a much more intense and broader band at ∼670 nm. Since the former band lies lower in energy than P680, the absorption band of the primary donor of the RC, the state(s) responsible for the 682−683 nm band could be referred to as a "red" antenna state as are frequently the lowest energy Q_y-antenna states of PSI.[21,22] As discussed in ref 21, however, whether an antenna state lies lower in energy than the primary donor state should be determined on the basis of site excitation distribution functions (SDF) rather than absorption maxima. In the case of CP47, spectral hole burning experiments led to identification of red states at 684, 687, and 690 nm.[23] The most detailed low-temperature spectroscopic study of CP43 is that of Groot et al.[24] who employed triplet-minus-singlet, fluorescence line narrowing (FLN), linear and circular dichroism spectroscopies, as well as Stark modulation spectroscopy. They identified two states at 679.6 and 682.5 nm whose FLN spectra exhibited significant differences in vibronic structure. The widths of the Q_y-bands of these two states are ∼210 and 60 cm^{-1}. However, Groot et al. emphasized that there is considerable uncertainty in the location and width of the higher energy band since their values were obtained by fitting the Q_y-absorption spectrum with several Gaussians. Their Stark modulation spectra led to a value for the permanent dipole moment change ($\Delta\mu$) associated with the absorption transition to the 682.5 nm state of ∼0 D.

The nonphotochemical hole burned (NPHB) and triplet bottleneck hole burned (triplet minus singlet) spectra as well as the zero-phonon hole (ZPH) action spectrum and Stark hole burning data presented in this paper directly identify two quasi-degenerate states at 682.9 and 683.3 nm. These states are referred to as B and A, respectively. Their Q_y-absorption bands and SDF are completely characterized. The electron−phonon coupling of both states is weak which, together with their small permanent dipole moment changes and other results, indicate that both are highly localized on a single (but different) Chl *a* molecule. The temperature dependence of the widths of the ZPH lead to the result that the natural radiative lifetime of both states is ∼8 ns. Furthermore, the kinetics of the A → B and B → A EET processes are found to be surprisingly slow, rate constants ∼$(6\ ns)^{-1}$. These results are discussed in the context of available structural information. It is concluded that the B state is the primary trap for EET from higher energy Q_y-states. The interesting question of why CP43 possesses two quasi-degenerate trap ("red") antenna states that are so weakly coupled is considered.

2. Materials and Methods

A. Preparation of CP43 Antenna Complex. The procedure for isolation of the CP43 complex from spinach was a modification of that reported by Alfonso et al.[19] and Groot et al.[24] The pigmented material that did not bind to the DEAE-Fractogel TSK 650s anion-exchange column was then passed through an S-Sepharose cation-exchange column equilibrated with buffer containing 20 mM Bis-Tris, pH 6.0, 20 mM NaCl, 10 mM $MgCl_2$, 0.03% (w/v) *n*-dodecyl β-D-maltoside (DM), and 1.5% (w/v) taurine at 22 °C. This column binds 22- and 10-kDa protein contaminants. The material that passed through the column was loaded onto a Q-Sepharose anion-exchange column at 4 °C equilibrated with the same buffer. Under these conditions, a 28-kDa contaminant protein binds to the column. The pigmented material that passed through the column was dialyzed overnight at 4 °C against 20 mM Tris-HCl (pH 7.8) plus 0.03% (w/v) DM and then loaded onto a second Q-Sepharose anion-exchange column equilibrated at 4 °C with the same dialysis buffer. The loaded column was subsequently washed with the dialysis buffer until the new eluate became colorless. The material remaining on the column was finally eluted with a 10−70 mM $MgSO_4$ linear gradient in the dialysis buffer. The eluted pigmented material (CP43 complex) exhibited a room-temperature absorption spectrum with a prominent red peak at 670 nm and a pronounced shoulder at 683 nm. This material was dialyzed twice for 2 h against 1 L of 20 mM Bis-Tris, pH 6.0, plus 0.03% DM; concentrated with 30-kDa cutoff Amicon Centricon tubes; and kept frozen at −80 °C until use. The final optical density at room temperature was close to 1.0 absorption units at 670 nm. All procedures were carried out in dim light at 4 °C. Concerning possible contamination by the CP47 core antenna complex, we note that our 4.2 K absorption spectrum of CP43 is very similar to that of Groot et al. who reported that[24] their samples were free of CP47. Additionally, the fluorescence origin band of CP47 at ∼691 nm[23] is absent in the fluorescence spectra of CP43 reported here. We are confident, therefore, that our samples are, for all intent and purposes, free of CP47. The samples were diluted for the low-temperature spectroscopic experiments. Glycerol was added (70% v/v) to ensure good glass formation.

B. Spectroscopic Measurements. The hole burning setup used is described elsewhere.[25−27] Absorption and hole burned spectra were recorded with a Bruker HR120 Fourier transform spectrometer at a resolution of 4 and 0.5 cm^{-1}, respectively. A Coherent CR699-21 ring dye laser (line width of 0.07 cm^{-1}), pumped by a 6 W Coherent Innova argon ion laser, was used for hole burning. The persistent nonphotochemical hole burned spectra reported correspond to the post-burn absorption spectrum minus the pre-burn absorption spectrum. The triplet bottleneck (transient) hole spectra correspond to absorption spectrum with laser on minus the spectrum with laser off. Burn intensities and times are given in the Figure captions. The sample temperature was maintained at 4.2 K using a Janis 8-DT Super Vari-Temp liquid helium cryostat, unless otherwise specified. Low-temperature fluorescence spectra were obtained using a Coherent UV argon-ion laser operating at 351.1 and 514.5 nm. Fluorescence was dispersed at a resolution of 0.8 nm by a McPherson 2061 1-m focal length monochromator and detected by a Princeton Instruments IRY 1024/G/B intensified photodiode array operated in CW mode of detection. Spectral resolution for fluorescence spectra was 0.3 nm. Care was taken to ensure that reabsorption effects were negligible.

Stark hole burning experiments and measurements of temperature-dependent holewidths were performed in the fluorescence excitation mode using an apparatus described in refs 28 and 29. A Coherent 699-29 Autoscan ring dye laser with line width of <20 MHz was used for excitation. Fluorescence was detected by a GaAs photomultiplier tube (RCA C31034) and a photon counter (SR-400, Stanford Research Systems, Sunnyvale, California). Scattered laser light was eliminated with cutoff filters at 750 nm. Laser intensities used for hole burning were in the range ∼10 $\mu W/cm^2$ and hole depths were typically less than 20%. For hole reading, the duration of which was about 300 s, the laser was attenuated by a factor of ∼60.

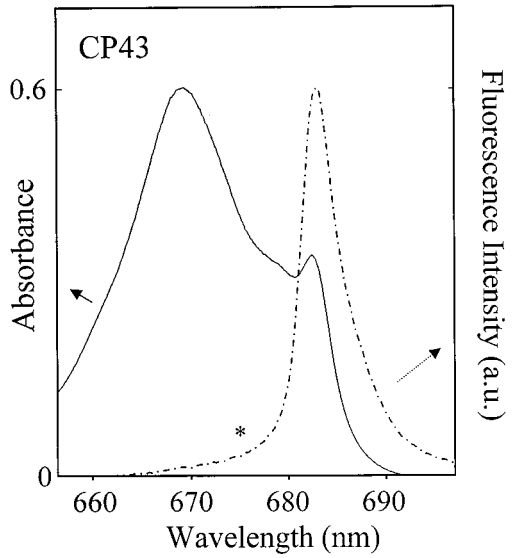

Figure 1. Absorption (solid line) and fluorescence (dash−dot line) of the CP43 complex obtained at 4.2 K. An excitation wavelength of 351.1 nm was used to obtain the fluorescence spectrum. The maximum of the fluorescence is at 683.1 nm.

A Trek Inc. model 610 C dc high-voltage power supply (Medina, New York) was used to generate the Stark field. A maximum Stark field of 10 kV/cm was applied since the zero-phonon holes were very narrow, ∼1 GHz. The gelatin capsule containing the sample was allowed to soften at room temperature for 5 min prior to being squeezed into the space between the electrodes. To avoid dielectric breakdown, all measurements were performed at 1.8 K in a Janis 10 DT liquid helium cryostat. The Stark cell consisted of two vertical Teflon walls and two copper electrodes perpendicular to the walls.[30,31] A separation distance of 5 mm (±0.05 mm) between electrodes was maintained by placing them into the grooves on the inside of the Teflon walls. A slit was made on one of the walls to allow laser beam access to the sample. A polarizer and polarization plane rotator placed in front of the Stark cell allowed for control of the laser polarization relative to the applied field direction (see ref 31 for details). Fluorescence was collected at a 90° angle relative to the incident laser light through an opening in the Stark cell.

3. Results and Discussion

A. Absorption and Fluorescence Spectra of CP43. The 4.2 K Q_y-absorption spectrum of CP43 shown in Figure 1 is very similar to that of Groot et al.[24] with an unusually sharp band at 682.4 nm, a more intense and broader band at 669 nm and a shoulder at ∼678 nm. The low-temperature spectra of refs 17−20 are similar but exhibit stronger absorption at ∼675 nm, as is the case for spectra obtained earlier in this laboratory for CP43 samples prepared by a different isolation and purification procedure (results not shown). The enhanced 675 nm absorption is probably due to a contaminant. The second and fourth derivatives of the absorption spectrum shown in Figure 1, when modeled, indicated that there may be two states absorbing near 683 nm (results not shown). That this is the case is confirmed by the results presented in the rest of this section.

The fluorescence spectrum shown in Figure 1 was obtained with an excitation wavelength of 351.1 nm for a sample with a detergent (DM) concentration of 0.03%. The maximum of the origin band is at 683.1 nm, which is close to the value reported by Groot et al.[24] That the maxima of the lowest energy absorption band at 682.4 nm and fluorescence origin at 683.1 nm are nearly coincident signifies that the electron−phonon coupling associated with the emitting state(s) is very weak. Further discussion of the weak coupling is given in subsection G. As a rule, the electron−phonon coupling of the Q_y-states of antenna complexes is weak.[32] The interested reader is referred to papers on the LHC II[33] and CP29[34] antenna complexes of PSII for recent examples of weak coupling. The only exceptions to the above rule we are aware of are the red antenna states of PSI of green plants and cyanobacteria.[35] The fluorescence spectrum of CP43 is discussed in more detail in subsection G.

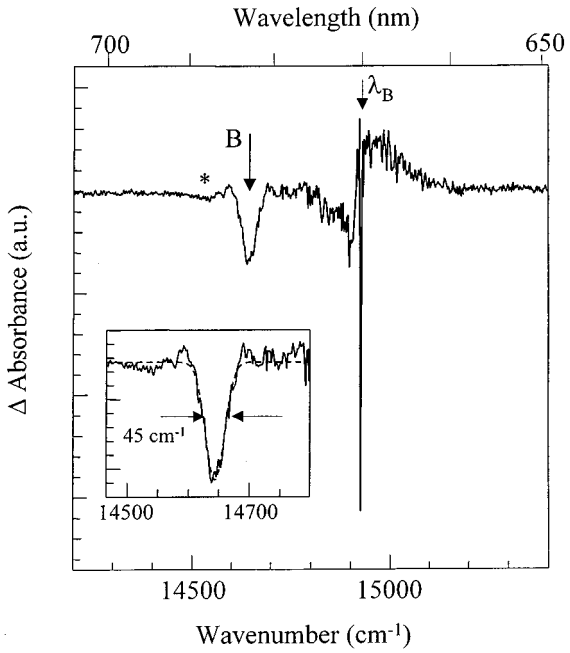

Figure 2. The 4.2 K persistent nonphotochemical hole burned (NPHB) spectrum of CP43 obtained with a burn wavelength (λ_B) of 670.0 nm, burn intensity = 500 mW/cm^2 and burn time = 60 s (burn fluence ∼ 30 J/cm^2). The read resolution used was 1 cm^{-1}. The fractional hole depths ($\Delta A/A$) of the zero-phonon hole at λ_B and hole B are 0.09 and 0.04, respectively. The inset shows a Gaussian fit to hole B at 682.9 nm with a fwhm = 45 cm^{-1}. The profile of hole B reflects the Q_y-absorption band of the B state.

B. Assignment of the Two Lowest Q_y-States of CP43. Persistent nonphotochemical hole burned (NPHB) spectra were obtained with several burn wavelengths (λ_B) $\lesssim$ 680 nm. The spectrum in Figure 2 was obtained with λ_B = 670.0 nm and a burn fluence of 30 J/cm^2. The positive increase in absorbance to the right of the zero-phonon hole (ZPH) at λ_B is the blue shifted anti-hole due mainly to the pseudo-phonon sideband hole (PSBH) that is located to the immediate left of the ZPH. The feature of primary interest is the low energy satellite hole labeled as B at 682.9 nm. Its position and shape were observed to be independent of λ_B. Thus, it is not a vibronic satellite hole. Therefore, it must be due to hole burning in a state (B) following its population by excitation energy transfer (EET) from states excited at λ_B. This is a common phenomenon in photosynthetic complexes (for recent examples see refs 33−35). That the wavelength of hole B, 682.9 nm, is close to the 682.4 nm wavelength of the lowest energy absorption band (Figure 1) establishes that the B state contributes significantly to the 682.4 nm band. The inset of Figure 2 shows a Gaussian fit to hole B with a full-width at half-maximum (fwhm) of 45 cm^{-1}. Since the site excitation distribution functions (SDF) of different Q_y-states are generally uncorrelated (for recent examples see refs 21, 33, and 34), and the profile of hole B is invariant to λ_B, it may be concluded that it is an accurate reflection of the B

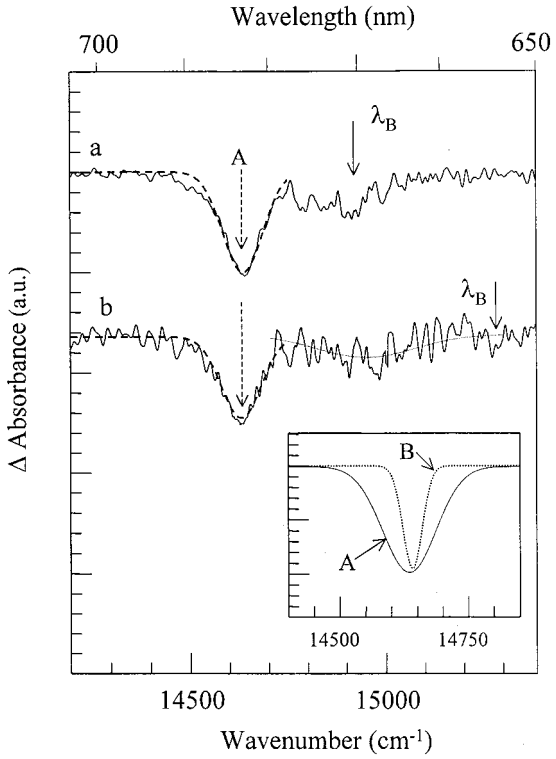

Figure 3. Triplet bottleneck hole spectra of CP43 obtained at 4.2 K with $\lambda_B = 670.0$ nm and burn intensity = 200 mW/cm^2 (spectrum a) and $\lambda_B = 655.0$ nm and burn intensity = 280 mW/cm^2 (spectrum b). The read resolution = 1 cm^{-1}. The profile of the A hole reflects the Q_y-absorption band of the A state. The dashed curves are Gaussian fits to hole A at 683.3 nm whose fwhm = 120 cm^{-1}. The inset compares the A (solid line) and B (dotted line) holes.

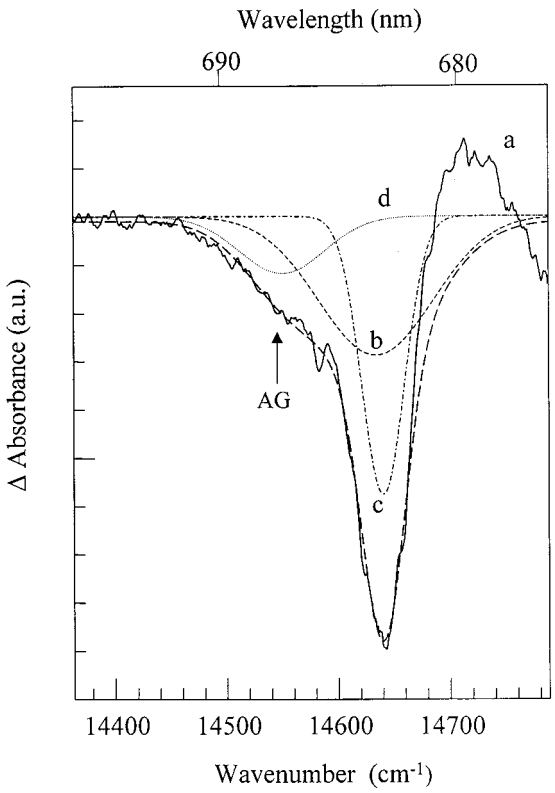

Figure 4. The 4.2 K saturated NPHB spectrum of CP43 (noisy curve a) obtained with $\lambda_B = 670.0$ nm, burn intensity = 200 mW/cm^2 and burn time = 75 min (burn fluence = 900 J/cm^2). Curves b and c are the Gaussian profiles of the A and B holes determined by the results in Figures 3 and 2, respectively. The shoulder indicated by AG is due to CP43 aggregates (see text). The profile of AG is curve d. The intensities of curves b, c, and d were adjusted to provide a good fit (long dashed curve) to the main part and low energy side of the experimental hole. The poor fit on the high energy side is due to the anti-hole which was not taken into account in the fitting.

absorption band. The asterisk in Figure 2 locates a weak satellite hole which may be due to aggregate formation (cf. subsection G).

Figure 3 shows 4.2 K triplet bottleneck hole spectra obtained with $\lambda_B = 670.0$ nm (a) and 655.0 nm (b). Both exhibit a hole (A) at 683.3 nm with a fwhm of 120 cm^{-1}. Since this width is much broader than the 45 cm^{-1} width of hole B, hole A is most likely due to a second Q_y-state located at 683.3 nm which will be referred to as the A state. The profiles of holes A and B are compared in the inset and, again, can be viewed as reflections of the A and B absorption bands. That they are symmetric is consistent with the electron−phonon coupling of the A and B states being weak. Further support for the existence of two quasi-degenerate states near 683 nm is provided by the highly structured fluorescence line-narrowed spectra of Groot et al.,[24] specifically their dependence on excitation wavelength in the vicinity of 683 nm.

The broad and relatively weak holes near 670 nm that lie to the blue of hole A in Figure 3 are discussed in subsection E in the context of excitonic couplings.

The results in Figures 2 and 3 raise the question as to why only the B state contributes to the NPHB spectrum and only the A state contributes to the triplet bottleneck spectrum (a weak contribution from the B state to this spectrum cannot be excluded). A plausible answer to the last part is that the intersystem crossing quantum yield of the singlet A state is higher than that of the B state and/or that the lifetime of its corresponding lowest energy triplet state is longer than that of the triplet state associated with the singlet B state. In this regard, the preliminary 5 K results reported in[24] are relevant since they identify two triplet states with lifetimes of ∼0.6 ms and 2.7 ms that elicit, respectively, a dominant bleach (hole) in the Q_y-absorption spectrum at 683 nm and a minor bleach at 684 nm. However, if the former bleach corresponds to the A state, the intersystem crossing yield of that state would have to be much higher than that of the B state. Clearly, more detailed experiments of the type briefly reported on in ref 24 are required to establish the connection between the A and B states and the above two triplet states. The two most apparent answers to the first part of the above question related to NPHB is that the NPHB efficiency of B state is much higher than that of the A state or that the B state is the primary trap for EET from higher energy Q_y-states. The hole burning results presented later argue against the former possibility, leaving the latter as the more likely explanation.

With that in mind we performed NPHB experiments with burn fluences much higher than the fluence of 30 J/cm^2 used to obtain the spectrum in Figure 2, the rationale being that if hole B in Figure 2 was saturated, then NPHB of the A state might be observed. The spectrum shown in Figure 4 (curve a) obtained with a burn fluence of 900 J/cm^2 and $\lambda_B = 670.0$ nm is consistent with this reasoning. The saturated fractional hole depth is 0.15, which is a factor of 5 larger than that of hole B in Figure 2. The reason the saturated hole depth is only 0.15 is due to excitation of the anti-hole sites by downward EET which is essentially equivalent to light induced hole filling (LIHF), a well-known phenomenon.[36,37] That is, excitation of anti-hole sites return them to their pre-burn configurations which leads to hole filling. The equilibrium between hole burning and hole

TABLE 1: Values of Spectroscopic Parameters for the CP43 Core Antenna Protein of PS II in the low-temperature Limit

	absorption		SDF [a]	
band	maximum (nm) ±0.1 nm	fwhm (cm^{-1}) ±5 cm^{-1}	maximum (nm) ±0.1	fwhm (cm^{-1}) ±5 cm^{-1}
A	683.3	120	683.4	115
B	682.9	45	683.0	43

[a] SDF ≡ site-distribution function.

filling determines the saturated depth of the hole. This is consistent with the observation that fractional hole depths of 0.70 are observed when λ_B is located in the A and B absorption bands, vide infra. The maximum of the hole shown in Figure 4 is at ~683 nm, which is between the maxima of the A and B absorption bands at 683.3 and 682.9 nm. Furthermore, the width of the hole is ~70 cm^{-1} which is intermediate in value between the 45 and 120 cm^{-1} widths of holes B and A, Table 1. This suggests that the hole in Figure 4 is a superposition of holes A and B plus a third hole indicated by AG which is attributed to aggregate formation since its intensity depends on detergent concentration (data not shown but see subsection G). Curves b and c are the Gaussian profiles of holes A and B as determined by experiment, Table 1. Their intensities were varied along with the position, intensity and fwhm of the Gaussian for the AG hole to arrive at the overall fit (long dashed curve). The AG hole is at 687.3 nm and carries a width of 100 cm^{-1}. The fit at the peak and low energy side of the hole is satisfactory. The poor fit on the high energy is due to the anti-hole which was not taken into account in the fitting. We note that the intensities of the A and B holes obtained by fitting are comparable.

Turning next to Figure 5, curve a is the NPHB spectrum obtained with $\lambda_B = 683.0$ which is close to the maxima of the A and B bands. The fractional hole depth of the ZPH at λ_B is 0.18. To its immediate left and right is the pseudo-PSBH (long upward arrow) and real-PSBH indicated by the ω_m arrow. The peak phonon frequency (ω_m) is ≈15 cm^{-1}. The two short arrows locate another excited-state mode at 75 cm^{-1} which may correspond to the 86 cm^{-1} ground-state mode in the FLN spectra of Groot et al.[24] Spectrum b was obtained with $\lambda_B = 680.5$ nm (14 695 cm^{-1}). At this wavelength the B band is not pumped but the A band is on its high energy side, see insert of Figure 3. This higher energy excitation leads to formation of hole B which strongly indicates that the A state transfers energy to the B state. We note that such energy transfer is inconsistent with the interpretation that has the A and B states being the "same" trap state in two distinct types of CP43 complex that arise due to gross heterogeneity. It is also very difficult to understand why the spectroscopic properties and trapping efficiencies of the A and B molecules are so different. The broad, high energy satellite holes (dotted arrows) in Figure 5 are discussed in subsection E in the context of possible excitonic couplings.

The results in Figures 2−5 point quite convincingly to CP43 possessing two quasi-degenerate and lowest energy states (A and B) at 683.3 and 682.9 nm. The Stark hole burning results and ZPH action spectrum presented in the next two subsections provide strong additional evidence for their existence. In addition, they and other results indicate that both states are mainly localized on a single Chl *a* molecule.

C. Stark Hole Burning Results. Recently, Stark hole burning spectroscopy (SHBS) has been successfully applied to several photosynthetic complexes including the LH2 and LH1 antenna complexes of purple bacteria,[30,31] the Fenna-Matthews-Olson antenna complex of *Chlorobium tepidum*,[30] the LHC II antenna complex of PSII,[21] and PSI of *Synechocystis* sp 6803.[35] As discussed in ref 35, SHBS is a more powerful approach than classical Stark modulation (CSM) spectroscopy for the determination of the permanent dipole moment change of $S_0 \rightarrow Q_y$ chlorophyll transitions since it can be state selective. This advantage is particularly important when the Q_y-absorption spectrum is spectrally congested, as is the case for CP43. In ref 35, SHBS was used to identify the two lowest energy Chl *a* red antenna states of PSI whose ground-state absorption bands overlap to a significant extent. Stark spectroscopy is also important because the magnitude of the dipole moment change is related to the degree of charge-transfer character in the excited Q_y-states as first demonstrated for the special pair of the bacterial reaction center.[38]

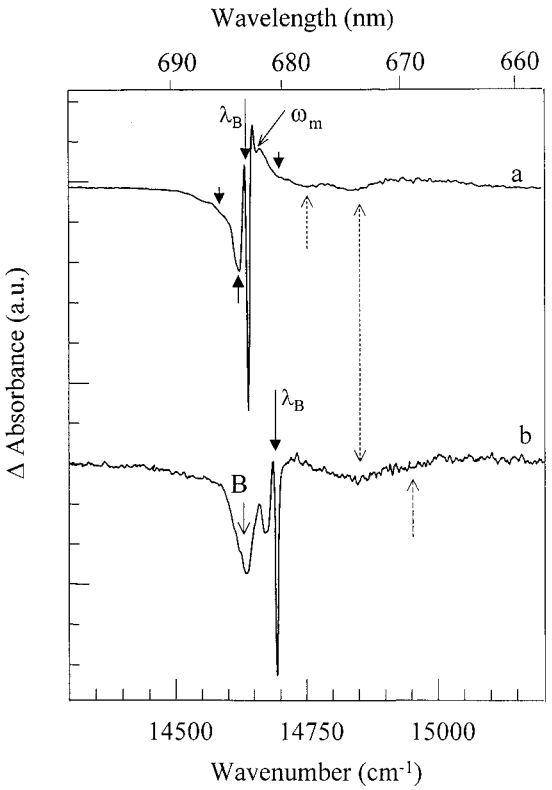

Figure 5. Persistent NPHB spectra of CP43. Spectrum a was obtained with $\lambda_B = 683.0$ nm, burn intensity = 250 mW/cm^2 and burn time = 600 s; spectrum b was obtained with $\lambda_B = 680.5$ nm, burn intensity = 125 mW/cm^2 and burn time = 800 s. The fractional hole depths of the ZPH at λ_B are, respectively, 0.24 and 0.12. The dotted arrows are high energy satellite holes due to excitonic couplings (see text). The ω_m arrow and short solid arrows locate the phonon sideband holes associated with the ZPH at λ_B.

The theoretical analysis of the SHBS results for CP43 that follows is identical to that of refs 30 and 31 which is based on the well-tested theory of Kador et al.[39] It was confirmed that at the low external (Stark) fields applied, the quadratic effect is negligible as was the case in our previous studies of photosynthetic complexes.[31] Thus, eq 1 given below which was used to analyze the Stark data for CP43 describes the Stark broadening of the ZPH due to the linear Stark effect which applies when the frequency shift of the zero-phonon line varies linearly with the applied Stark field (E_S).[39]

Frames A and B of Figure 6 show the Stark broadening of a ZPH burned at $\lambda_B = 683.0$ nm (14 641 cm^{-1}) and at 686.0 nm (14 577 cm^{-1}), respectively, for laser polarization perpendicular to the applied field. We emphasize that the former wavelength is close to the maxima of the A and B bands and thus, both the A and B states are excited. (In the following subsection it is

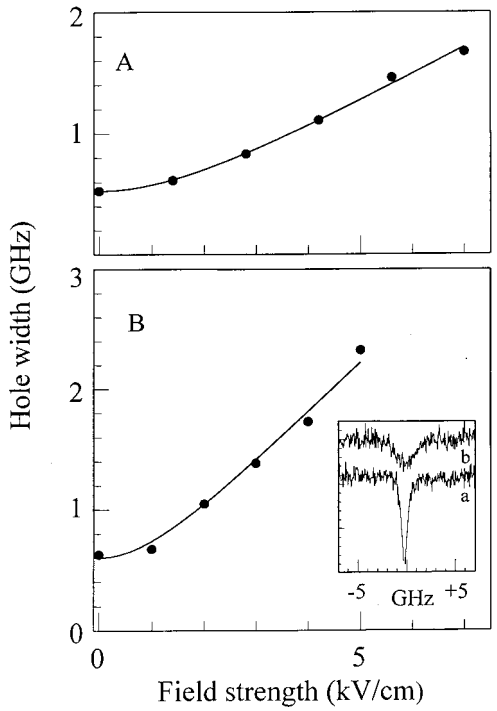

Figure 6. Dependence of the zero-phonon holewidth on external electric field obtained at 1.8 K with $\lambda_B = 683.0$ nm (frame A) and $\lambda_B = 686.0$ nm (frame B) and laser polarization perpendicular to the applied field. The solids are fits obtained using eq 1 which yielded $f \cdot \Delta\mu_\perp = 0.23 \pm 0.5$ D (frame A) and $f \cdot \Delta\mu_\perp = 0.43 \pm 0.5$ D (frame B), values that are very similar to those obtained with parallel polarization (see text). The inset shows the ZPH at zero applied field (a) and at 5 kV/cm (b).

confirmed that both states lead to NPHB.) On the other hand, irradiation at $\lambda_B = 686.0$ nm is too low in energy to excite the B state; only the A state is excited, see insert in Figure 3. Clearly, the Stark broadening effect is much stronger for $\lambda_B = 686.0$ nm. (The insert in frame B shows ZPH holes obtained at zero applied field and at a field strength of 5.0 kV/cm^2). The solid curves through the data points are fits obtained using

$$\Gamma(F) = 2\gamma(1 + F^2)^{1/2} \quad (1)$$

where $\Gamma(F)$ is the Stark broadening and

$$F = 4\pi f \cdot \Delta\mu E_S/\hbar\gamma \quad (2)$$

In eq 2 $\Delta\mu$ is the permanent dipole moment change, f is the local field correction, E_s is the applied field strength, and γ is the fwhm of the ZPH at zero applied field. The dipole moment change $\Delta\mu = \Delta\mu_0 + \Delta\mu_{ind}$, where $\Delta\mu_0$ is the molecular dipole moment change and $\Delta\mu_{ind}$ is the change induced by the internal electric field of the protein (E_{int}). When the polarizability difference tensor, $\Delta\alpha$, is that of an isotropic medium, $\Delta\mu_{ind} = \Delta\alpha E_{int}$. For CP43, Stark splitting of the ZPH was *not* observed for laser polarization parallel or perpendicular to E_s, only Stark broadening. As discussed by Gafert et al.[40] this means that $\Delta\mu$ is dominated by $\Delta\mu_{ind}$ and that the sense of $\Delta\mu_{ind}$ is not well-defined, i.e., it is essentially randomly distributed. The only photosynthetic complex for which Stark splitting has been observed is the Fenna-Matthews-Olson complex.[30]

The fits shown in Figure 6 for laser polarization perpendicular to the applied field result in $f \cdot \Delta\mu_\perp = 0.23 \pm 0.05$ D and 0.43 ± 0.05 D for $\lambda_B = 683.0$ D and 686 nm, respectively. The results for laser polarization parallel to the applied field (not shown) led to $f \cdot \Delta\mu_{||}$ values of 0.26 ± 0.05 D and 0.51 ± 0.05 D, respectively. That the dipole moment changes for parallel and perpendicular laser polarizations are nearly equal indicates that the polarizibility difference tensors are quite isotropic. The average values of $f \cdot \Delta\mu_{||}$ and $f \cdot \Delta\mu_\perp$ are given in Table 2 where they are compared with $f \cdot \Delta\mu$ values obtained by SHBS for Chl *a* in other photosynthetic complexes.

TABLE 2: Stark Hole Burning Results (unless otherwise specified[a]) for CP43 Antenna Protein Complex and Other Systems Containing Chl *a*

system	λ_B, nm	$(f \cdot \Delta\mu)^b$(D)	reference
CP43	683	0.25 ± 0.05	this work
	686	0.47 ± 0.05	this work
	680	0.3[a]	24
	683	0[a]	24
Chl *a*: PVB	666	0.52 ± 0.05	21
Polymer films	674	0.52 ± 0.05	21
Chl *a*: LHC II	680	0.63 ± 0.10	21
Chl *a*: PS II RC	670	0.50 ± 0.05	21
+ Triton X-100	672	0.49 ± 0.05	21
PSI of *Synechocystis*	714	2.3 ± 0.2	21

[a] Values obtained using classical Stark modulation spectroscopy. [b] The average of the $(f \cdot \Delta\mu_\perp + f \cdot \Delta\mu_{||})$ values; see text for $f \cdot \Delta\mu_\perp$ and $f \cdot \Delta\mu_{||}$ values.

The *key finding* is that the average value of 0.47 D of $f \cdot \Delta\mu$ for $\lambda_B = 686.0$ nm is a factor of 2 larger than the value of 0.25 D for $\lambda_B = 683.0$ nm. (We remind the reader that with $\lambda_B = 686.0$ nm the B state is not excited, only the A state.) This difference cannot be explained under the assumption that the 682.4 nm absorption band seen in Figure 1 is due to a single state and that the factor of 2 difference is due to the dependence of the dipole moment change on the location of λ_B within the inhomogeneously broadened 682.4 nm absorption band. Such a dependence leads to a variation in $\Delta\mu$ of only a few percent. In the cases of the lowest exciton levels of the BChl *a* LH1 and LH2 rings of purple bacteria[30] and three lowest exciton levels of the Fenna-Matthews-Olson antenna complex, no such dependence was observed.[30] In other words, the above factor of 2 is large and cannot be explained unless there are two states (A and B) that contribute to the 682.4 nm absorption band. We conclude that the average value of $f \cdot \Delta\mu$ for the A state is 0.47 D and that the value for the B state is close to 0.25 D.

It is instructive to compare these values with those obtained for Chl *a* molecules in other systems, Table 2. For Chl *a* in poly(vinyl butyral) films and in the PSII reaction center in the presence of the detergent Triton X-100, one is dealing with monomer Chl *a*. (This detergent leads to unconnected Chl *a* molecules absorbing near 670 nm.) The value of 0.63 D for LHC II of PSII is that of its lowest energy state which is highly localized on a single Chl *a* molecule that is weakly coupled to other Chl molecules in the complex.[33] Thus, it was concluded that[21] $f \cdot \Delta\mu$ for an isolated Chl *a* molecule in proteins is $\approx$0.5 D. In all three systems $\Delta\mu$ is dominated by $\Delta\mu_{ind}$ and the electron−phonon coupling is weak ($S < 1$), as is the case for the A and B states, vide infra. This weak coupling and the Stark results are consistent with the Chl *a* molecules responsible for the A and B states being weakly coupled to other Chl *a* molecules (see also subsection E). We note that Groot et al.[24] estimated that the intensity of the 682.4 nm absorption band is equivalent to that of $\sim$1 Chl *a* molecule under the assumption that CP43 contains 14 Chl *a* molecules. In the following subsection an estimate of 1.7 Chl *a* molecules for the combined intensity of the A and B bands is arrived at. In sharp contrast to the small $f \cdot \Delta\mu$ values just discussed, the value of 2.3 ± 0.2 D for the lowest energy red antenna state at 714 nm of PSI

(*Synechocystis* sp. PCC 6803) is large, only a factor of 2 lower than the value for the special pair state (P870*) of the bacterial reaction center of *Rhodobacter sphaeroides*. As mentioned earlier, the electron−phonon coupling of the 714 nm state is strong with a total Huang−Rhys factor of 2.0 due to modes at 18 and 70 cm^{-1}.[35] Furthermore, the linear pressure shift rate of -0.5 cm^{-1}/MPa for the 714 nm state is significantly larger than the ≈ -0.1 cm^{-1}/MPa value for monomer-like Q_y-states.[41−43] It was concluded that[35] the 714 nm state is due to a dimer of strongly coupled Chl *a* molecules and, furthermore, that it possesses significant charge-transfer character.

In summary, the Stark hole burning results for the isolated CP43 complex provide convincing proof of the existence of the quasi-degenerate A and B states. The small $f \cdot \Delta\mu$ values for the two states indicate that their associated Chl *a* molecules are not strongly coupled with other Chl *a* molecules. In subsection E data are presented which show that the coupling between the Chl *a* molecules of the A and B states is extemely weak.

D. The Zero-Phonon Hole Action Spectrum in the Vicinity of 683 nm. In ZPH action spectroscopy one burns holes at different λ_B-values under constant burn fluence conditions. The Δ-absorbance values at the peaks of the ZPH plotted versus λ_B is the ZPH action spectrum. The action spectrum reflects the Gaussian site distribution functions (SDF) of the contributing states. This type of spectroscopy was introduced in ref 44 where it was used to identify and characterize the lowest exciton level of the LH1 antenna complex of *R. sphaeroides*. Since then it has been successfully applied to several isolated photosynthetic complexes.[42−50] The emphasis in those works was mainly to identify and characterize the Q_y-states that contribute to the low energy part of the Q_y-absorption spectrum.

The ZPH action spectrum for isolated CP43 obtained with a burn fluence of 0.5 J/cm^2 is shown in Figure 7 (solid diamond data points). The fractional hole depth of the deepest ZPH was 0.12. The holewidths were determined by the read resolution of 0.5 cm^{-1} (the actual holewidths are much narrower, see following subsection). The action spectrum was scaled so as to provide a fit to the low energy side of the 682.4 nm band of the absorption spectrum (somewhat noisy solid curve). The short dashed curve and the dotted curve are the SDF of the A and B states that, in combination, provide a good fit (long dashed curve) to the main part and low energy side of the action spectrum. Their peak positions and widths are given in Table 1. That they differ only slightly from the values for the A and B absorption bands was expected since the electron−phonon coupling for the A and B states is weak. The fit fails at the high energy side of the action spectrum as indicated by the X. In our earlier studies of CP43 isolated and purified by a different procedure the X-region of the action spectrum was considerably more intense than seen in Figure 7 (unpublished results). This increase in intensity was accompanied by an increase in absorption intensity near 675 nm. Thus, the X-region seen in Figure 7 is most likely due to a minor contaminant.

On the basis of the deconvolution shown in Figure 7 we estimated that the combined contribution of the A and B bands to the Q_y-absorption spectrum is (12 ± 2)% (integration of the absorption spectrum was cut on the high energy side at 655 nm). For a content of 14 Chl *a* molecules, the combined contribution is equivalent to the absorption of 1.7 ± 0.2 Chl *a* molecules. Given that the vibronic contributions of the A and B molecules to the Q_y-spectrum were not taken into account in the calculation, we believe that the combined contribution is most likely that of two Chl *a* molecules.

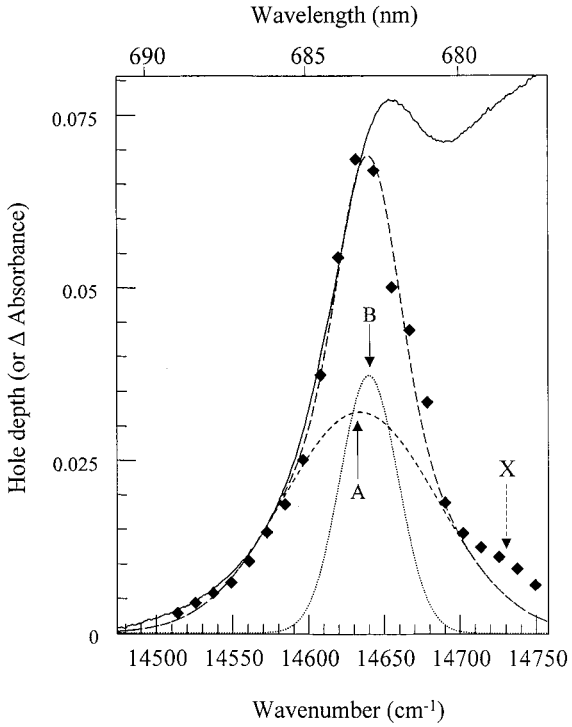

Figure 7. Zero-phonon hole action spectrum of CP43 obtained at 4.2 K with a constant burn fluence of 0.5 J/cm^2. Read resolution = 0.5 cm^{-1}. Solid diamonds are the Δ-absorbance changes of the ZPH. The solid curve is the experimental absorption spectrum. The long dashed curve is the best fit to the action spectrum obtained using the SDF of the B state (dotted curve) and the A state (short dashed curves). The maxima and widths of the SDF are given in Table 1. Note that their values are very similar to those of the A and B absorption bands, a consequence of weak electron−phonon coupling. See text for discussion of feature X.

To conclude this subsection we note again that Groot et al.[24] identified two states at 679.6 and 682.5 nm with ground-state absorption bandwidths of ∼200 and ∼60 cm^{-1}, respectively. There is no doubt that their 682.5 nm state corresponds to our B state. They pointed out that the location of the other state is quite uncertain due to arbitrariness in the fitting of the Q_y-absorption spectrum. It is possible that their 679.6 nm state corresponds to our 683.3 nm A state.

E. Coupling and Energy Transfer between the A and B States. The existence of the two lowest energy and quasi-degenerate A and B states at 683.3 and 682.9 nm, respectively, raises a number of interesting questions that are addressed in this subsection, including the strength of the coupling between the Chl *a* molecules of the two states and the A ↔ B transfer rates. The data used are the ZPH widths obtained in the fluorescence excitation mode with a resolution <20 MHz and λ_B-values in the vicinity of the A and B bands.

Before presenting the holewidth results it is instructive to consider first the low-temperature absorption profiles of the A and B bands shown in the inset of Figure 3, where the broad and narrow profiles correspond to A and B, respectively. As discussed, these profiles are essentially the SDF of the A and B states. One sees immediately that in the low-temperature limit A → B and B → A EET in significant fractions of the complexes in a bulk sample would be energetically forbidden. (Furthermore, the energy ordering of the A and B states from complex to complex can be different since the SDF of different Q_y-states are generally uncorrelated.) Spectrum b of Figure 5 shows that this is the case for CP43. It was obtained with λ_B = 680.5 nm which does not lead to excitation of the B state, only excitation

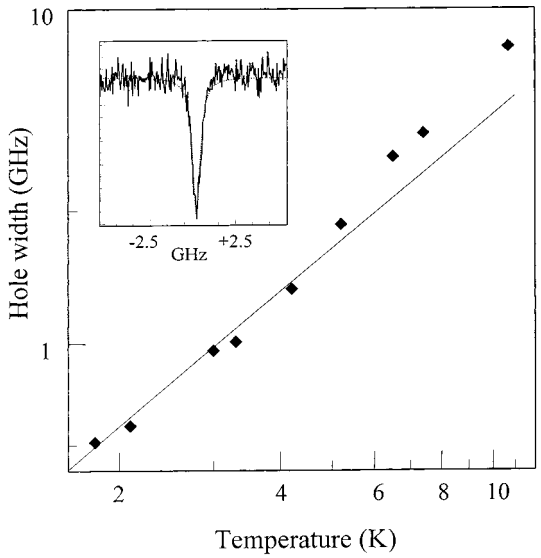

Figure 8. Temperature dependence of the ZPH width (solid diamonds) for $\lambda_B = 685.0$ nm. At this wavelength only the A state is excited. The solid line is the fit obtained with eq 3 using data for $T < 6$ K. See text for discussion.

of the A state. If the SDF of these two states were perfectly correlated, hole B would be about as sharp as the ZPH at λ_B, which is clearly not the case. Very recently the situation in the insert of Figure 3 was shown to exist in PSI of *Synechocystis*, where the narrow and broad SDF are those of P700 and the second lowest energy red antenna state, respectively.[35] This finding led to an explanation of why only about 50% of the PSI reaction centers undergo irreversible charge separation in the low-temperature limit.[35] At room temperature, EET between the A and B states of CP43 would be expected to occur in all complexes since $kT \sim 200$ cm^{-1}.

The dependence of the width of a ZPH burned at 685.0 nm (14 599 cm^{-1}) on temperature is shown in Figure 8. Excitation of the B state with this wavelength is not possible while excitation of the A state is, see insert of Figure 3. The insert in Figure 8 shows the ZPH hole (fractional hole depth of 0.1) at $T = 1.8$ K, the lowest temperature used. The profile is well described by a Lorentzian with a width of 0.54 GHz (0.018 cm^{-1}). The same width at 1.8 K was obtained with $\lambda_B = 686.0$ nm. The uncertainty in the holewidths was estimated at ±5%. In the absence of dynamical processes that lead to hole broadening on a time scale longer than the excited-state lifetime,[51] the homogeneous width of the zero-phonon line (ZPL) is $2(T_2^{-1})$, where T_2 is the total dephasing time. The latter is defined as $(T_2)^{-1} = (2T_1)^{-1} + T_2^{*-1}$, where T_1 is the excited-state lifetime and T_2^* is the pure dephasing time. The holewidth (twice the width of the ZPL) of 0.54 GHz results in $T_2(1.8\text{ K}) = 1.2$ ns.

The solid line in Figure 8 is the fit to the data points for temperatures lower than 6 K obtained using

$$\Gamma(T) = \Gamma_0 + AT^{\alpha} \qquad (3)$$

where $\Gamma(T)$ is the holewidth and Γ_0, which is temperature independent, is the width in the limit as $T \rightarrow 0$ K. The fit yielded $\Gamma_0 = 40 \pm 5$ MHz, $\alpha = 1.3 \pm 0.1$, and $A = 0.21$ GHz K$^{-1.3}$. The second term in eq 3 is the contribution from the coupling between the optical transition and the glasslike two-level systems of proteins. This coupling has been thoroughly studied in many chromophore/amorphous molecular host systems (see refs 51 and 52 for reviews). Generally, it is found that α is close to 1.3, a value that is theoretically understood (see ref 53 and references therein). The $T^{1.3}$ behavior, which typically dominates the spectral dynamics at temperatures lower than ≈10 K, has recently been observed for several isolated photosynthetic systems.[33,34] For the three lowest Q_y-states of the Fenna-Matthews-Olson trimer complex from *Chlorobium tepidum* and *Prosthecochloris aestuarii*, $A = 0.21$ and 0.18 GHz K$^{-1.3}$, respectively.[54] The three highest temperature data points in Figure 8 indicate the onset of a thermally activated dephasing process that involves low-frequency protein phonons. Such dephasing has been observed in other photosynthetic complexes.[33,34,46,52,54] More detailed holewidth measurements at temperatures considerably higher than 10 K are required for a detailed understanding of this dephasing process in CP43.

It is apparent that there is nothing unusual about the spectral dynamics of the A state of CP43. Although these dynamics are interesting and not understood in detail, the primary motivation for our holewidth measurements was to obtain data related to the time scale of EET between the A and B states. The value of $\Gamma_0 = 40$ MHz for the A state obtained with $\lambda_B = 685.0$ nm leads to a lifetime (T_1-value) of 8 ± 1 ns which is about the value expected for the radiative lifetime of a monomer-like Chl *a* Q_y-state (see ref 55 and references therein). This finding is consistent with the SDF of the A and B states since excitation at $\lambda_B = 685.0$ nm should only excite the A state of complexes incapable of undergoing EET to the B state. We then measured holewidths at 1.8 K for λ_B-values between 678.0 nm (14 749 cm^{-1}) and 683.0 nm (14 641 cm^{-1}) which, according to the inset of Figure 3, should lead to A → B and B → A EET. Interestingly, the holewidths were only slightly broader (10−20%) than the width of 0.54 GHz for the holes burned at 685.0 and 686.0 nm, (hole profiles not shown). The holewidth at 682.0 nm was 0.63 GHz. The assumption that this width is entirely due to EET leads to a rate constant of (1.0 ns)$^{-1}$. However, this assumption is highly questionable since the contribution from electron-TLS coupling to the width of the hole at 682.0 nm should be nearly the same as the contribution to the 685 nm holewidth which is 0.54 GHz. (This has been demonstrated for the three lowest energy Q_y-states of the Fenna-Matthews-Olson complex.)[54,56] Thus, an effective width of ∼0.1 GHz for EET is far more reasonable. It leads to an EET rate constant of only ∼(6 ns)$^{-1}$, essentially the same as the rate constant for radiative decay! The key point is that the A → B and B → A energy transfer processes are extremely slow. Therefore, the coupling between the Chl *a* molecules of the A and B states must be very weak which, in turn, means that the distance between the two Chl *a* molecules is probably comparable to the Förster radius of ≈30 Å for Chl *a*. It is also possible that the orientation of the transition dipoles is unfavorable for EET. We are reminded, however, that spectrum b of Figure 5 shows that the A state for a subset of complexes transfers energy to the B state. From the inset of Figure 3 it follows that the B state should also be capable of transferring to the A state. We emphasize that these transfer processes should also be unusually slow at biological temperatures.

F. Different Functions for the A and B Red Antenna States? To the best of our knowledge, CP43 is unique in that it possesses two monomer-like, quasi-degenerate red antenna states whose Chl *a* molecules are very weakly coupled and, therefore, spatially far removed from each other. In the preceding subsection it was concluded that the rates for EET between the A and B states are extremely low, ∼(6 ns)$^{-1}$. Furthermore, their natural radiative lifetimes are ≈8 ns which indicates that their intersystem crossing rates are not unusually fast. Both states

serve as traps for downward energy transfer from higher energy states. The question of why, in the evolutionary process, CP43 ended up with two quasi-degenerate antenna states whose Chl *a* molecules are so weakly interacting is interesting. We return to it at the end of this subsection after drawing some additional conclusions about the A and B states.

Argued first is that the hole spectra in Figures 2 and 4 establish that the primary trap state is the B state. They show that upon excitation of higher energy Q_y-states which populate the A and B states by downward energy transfer, production of the nonline narrowed B hole is far more efficient than that of the A hole. (The burn fluence used to detect the A hole in Figure 4 is a factor of 20 higher than that used to obtain the spectrum in Figure 2 which shows only the B hole.) The large difference in efficiency is not due to a difference in hole burning quantum yields since the ZPH action spectrum in Figure 7 shows that, upon direct excitation, the hole burning efficiencies of the two states are comparable and because their natural radiative lifetimes are very similar. We conclude, therefore, that the B state is the dominant trap state and is of primary importance in transferring energy to the reaction center. That the A state is a minor player in trapping raises the question of what its main function is, vide infra. The triplet bottleneck hole spectra in Figure 3 also show that the A state is populated by energy transfer from higher energy states. That the B state makes, at most, a small contribution to the hole spectra in that figure does not necessarily contradict the above conclusion since the contribution to the bottleneck spectrum (often referred to as the triplet−singlet spectrum) depends on the intersystem crossing yield and the lifetime of the triplet state, the values of which are not known for the A and B states.

As noted earlier, the fluorescence line narrowed (FLN) spectra of Groot et al.[24] obtained with excitation wavelengths in the vicinity of 683 nm firmly establish that there are two low energy emitting states with comparable fluorescence quantum yields. Given the results presented here, there is little doubt that their two states correspond to our A and B states. They suggested that the Chl *a* molecules responsible for the two states may belong to different pools. Our finding that the A → B and B → A energy transfer rates are exceedingly slow, $\approx(6\ \text{ns})^{-1}$, provides considerable support for their suggestion. The triplet bottleneck hole spectra in Figure 3 and NPHB spectra in Figure 5 provide additional support. Both spectra in Figure 3 exhibit, in addition to hole A, a relatively weak and broad hole at ~669 nm. These two holes also appear in the triplet bottleneck (triplet minus singlet) spectra obtained by Groot et al.[24] with excitation wavelengths between 660 and 670 nm. In agreement with Groot et al. we conclude that the higher energy hole is most likely due to a state(s) at 669 nm that is excitonically correlated with the A state. That is, the Chl *a* molecule mainly responsible for the A state (vide supra) contributes to the 669 nm state, albeit weakly given the weakness of the 669 nm hole. The optically detected magnetic resonance spectra (8 K) of Carbonera et al.[17] also revealed correlated bleaching near 683 and 668 nm. As discussed in subsection B, the top NPHB spectrum a in Figure 5 was obtained with excitation at 683.0 nm that populates both the A and B states. Two high energy satellite holes at 678 and 673 nm are apparent (dotted arrows). The 669 nm hole seen in Figure 3 is absent. We conclude, therefore, that the 678 and 673 nm holes are due to states that are excitonically correlated with the B state. An absorption band at 678 nm is evident in Figure 1. The λ_B-value of 680.5 nm used to obtain spectrum b in Figure 5 results in the population of the A state but not the B state, see subsection B. However, uncorrelated A → B energy transfer occurs that results in hole B. The 673 nm hole seen in spectrum a also appears in spectrum b, although its width in the latter spectrum would appear to be broader. The difference in widths may be due to the difference in the anti-hole profiles which interfere with the high energy satellite holes in the two spectra. This is probably the reason the 678 nm hole seen in spectrum a of Figure 5 that is correlated with the B state is not apparent in spectrum b. Because the shapes of the anti-holes are not known it is not possible to deconvolve the spectra to obtain the pure hole spectra. Finally, the dotted arrow in spectrum b of Figure 5 spectrum locates a weak feature that may be the 669 nm hole that correlates with the A hole in Figure 3. Interference of the 669 nm hole by the anti-hole associated with the 678 nm hole would mask its true intensity.

In summary, the A state appears to be excitonically correlated with a state(s) at 669 nm while the B state is correlated with states at 678 and 673 nm. The weakness of the satellite holes at these wavelengths suggest that the Chl *a* molecules of the A and B states are not strongly coupled with other Chl *a* molecules of CP43. As concluded earlier, the Chl *a* molecule of the A state and the Chl *a* molecule of the B state are very weakly coupled. This is consistent with the two Chl *a* molecules belonging to two different pools of Chl *a* molecules. On the basis of electron crystallographic data Rhee et al.[2] suggested that in CP47 two pools (layers), each containing ≈7 Chl *a* molecules, exist at opposite sides of the membrane. Given that both CP47 and CP43 possess six transmembrane α-helices with considerable homologies in their amino acid sequences, and that they possess ~14 Chl *a* molecules, it is likely that CP43 also possesses the two-layer motif.

To conclude this subsection we return to the question of why CP43 possesses the quasi-degenerate and very weakly interacting A and B states. Since our results establish that the latter is the primary trap state it stands to reason that its role in transferring energy to the reaction center is far more important than that of the A state. Based on the temperature-dependent absorption spectra of Groot et al.,[24] the location of the B state at room temperature is nearly the same as that at low temperatures, ~683 nm. Recent NPHB studies of the PSII reaction center at 4.2 K indicate that the Q_y-state of the peripheral Chl *a* molecule located on the D1 side is located near 684 nm.[46] This raises the interesting question of whether this peripheral state could serve to shuttle excitation energy from the B state to the primary donor of the reaction center. The unusually narrow width of the B band (45 cm^{-1}) at 4 K, together with the finding that the Chl *a* molecule associated with this band is weakly coupled with other Chl *a* molecules, suggests two things. First, the Chl *a* molecule is in a tight binding pocket and, second, that the low energy of its Q_y-state is mostly due to interaction with a specific protein residue. Accepting this, one might speculate that under conditions of photoinhibition, to which CP43 is sensitive (see Introduction), denaturation of CP43 could disrupt the tight binding pocket of the B state's Chl *a* molecule, thereby shifting its Q_y-state to higher energy so that it can no longer serve as a trap for energy transfer from higher energy Q_y-states.

We turn next to the question of what the function of the A state is. We have no data and are unaware of other data that speak to this question. It is possible that it simply serves to funnel energy to the reaction center but then one wonders why it is not nearly as effective a trap as the B state. We speculate that the main role of the A state may not be to transfer energy to the reaction center but rather to prevent efficient energy transfer to the reaction center. For example, the A state might be involved in the regulatory process that controls the amount

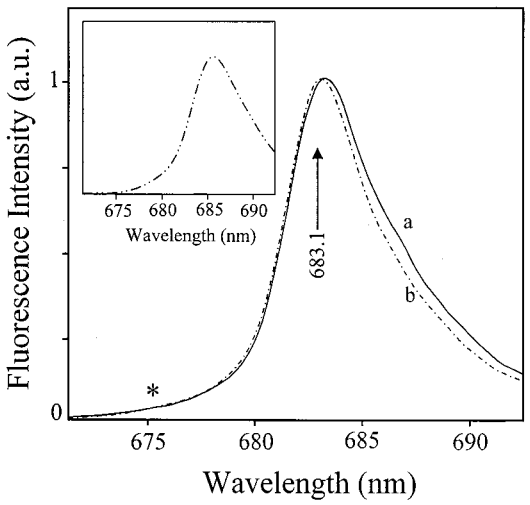

Figure 9. Normalized fluorescence spectra of the CP43 antenna complex at 4.2 K obtained with an excitation wavelength of 514.5 nm. Spectra a and b were obtained with 0.01% and 0.03% of DM, respectively. The inset shows a difference between spectra a and b (see text for details).

of excitation energy reaching the RC. This would mean that the Chl *a* molecule associated with the A state is far removed from the cofactors of the reaction center. It may be that the A state also has a role in the photoinhibition process. Experiments of the type reported here on CP43 isolated from photoinhibited PSII particles could test these ideas.

G. Fluorescence Spectra. Given that the B state is the primary trap one would expect that it should be the major contributor to the nonline narrowed fluorescence spectrum. That this is so is not immediately apparent since the width of the *asymmetric* fluorescence band at 683.1 nm in Figure 1 is 105 cm^{-1}, which is much broader than the 45 cm^{-1} width of the symmetric B absorption band, Figure 2. In the Condon approximation the width of the B state's fluorescence band should also equal 45 cm^{-1}. The tailing to the red of the fluorescence band in Figure 1 is unlikely to be due to the B state. Thus, a more reliable indicator of the B state's contribution is the half-width on the high energy side of the observed fluorescence band which is 40 cm^{-1}. However, the high energy side is interfered with by the fluorescence band indicated by the asterisk in Figure 1 (see also Figure 9). Modeling revealed that the maximum of this fluorescence band is at ~675 nm and that it carries a width of ~150 cm^{-1} (results not shown). It probably correlates with the feature in the ZPH action spectrum of Figure 7 indicated by X. Thus, the fluorescence at ~675 nm is probably due to a minor contaminant. Subtraction of the contribution of the ~675 nm band to the fluorescence spectrum reduced the above 40 cm^{-1} half-width to ~32 cm^{-1}. This width is much narrower than the half-width of 60 cm^{-1} expected for the A state's fluorescence band based on the 120 cm^{-1} width of the A absorption band, see Figure 3 and subsection B. We conclude, therefore, that the contribution from the A state to the 683.1 nm fluorescence band is considerably smaller than that of the B state. It is not possible to be quantitative since the shapes of the two fluorescence bands are unknown. In this regard we note that the monomer-like, lowest energy Q_y-state of the LHC II and CP29 complexes of PSII both exhibit a fluorescence origin band in the static spectrum that is ≈20% broader than the absorption origin band.[57] It was suggested that this mirror symmetry breakdown may be due to structural changes of the complexes that occur prior to fluorescence. It is reasonable to assume that such mirror symmetry breakdown exists for the A and B states.

The B absorption band is at 682.9 nm, Table 1. Thus, with the B state the major contributor to the central part of the fluorescence band at 683.1 nm, the Stokes shift is small, only 0.2 nm (4.4 cm^{-1}). This shift is, to a good approximation, given by $2S\omega_m$ where S is the Huang−Rhys factor and ω_m is the energy of the coupled phonons. Since the pseudo-PSBH is dominated by 15 cm^{-1} phonons (Figure 5) one arrives at a value of ~0.2 for S. A saturated fractional hole depth of 0.7 was measured at $\lambda_B = 683.0$ nm. An *upper limit* for S is obtained by setting this depth equal to $\exp(-S)$, which is the Franck−Condon factor for the ZPL.[58] The result is $S = 0.4$. Since the results in Figure 7 indicate that the intensities of the A and B bands at 683.0 nm are nearly equal and that the hole burning efficiencies and lifetimes of the A and B states are comparable it follows that 0.4 is an upper limit for S of both states.

To conclude this subsection we discuss the hole labeled as AG in Figure 4 whose maximum is near 687 nm. The hole spectrum was obtained for a sample with a detergent (DM) concentration of 0.03% as was the case for all hole spectra presented here. Clearly, a state at 687 nm cannot be intrinsic to the *isolated* CP43 complex. This leaves aggregate formation as the most likely explanation. With that in mind we studied the dependence of the nonline narrowed fluorescence spectrum on DM concentration. The excitation wavelength used was 514.5 nm. The spectra for DM concentrations of 0.01 and 0.03% are shown in Figure 9, curves a and b, respectively. The spectrum obtained with 0.05% DM was similar to spectrum b. The maximum of spectrum a relative to that of spectrum b is red-shifted by ~0.2 nm and its width is broader by ~20 cm^{-1}. The difference between the two spectra is shown in the insert. The maximum of the difference band (width ~ 135 cm^{-1}) is at 686 nm. At a DM concentration ≪0.01% the fluorescence maximum red-shifted to ≈687 nm. We conclude that the AG hole at 687 nm is due to aggregate formation. The red-shifting indicates that the Chl *a* molecule of the B state is located at the periphery of CP43. This is consistent with it playing an important role in transferring energy to the reaction center.

Acknowledgment. Research at the Ames Laboratory was supported by the Division of Chemical Sciences, Office of Basic Energy Sciences, U.S. Department of Energy. Ames Laboratory is operated for USDOE by Iowa State University under Contract W-7405-Eng-82. The assistance of H.-C. Chang during the initial phase of the research is gratefully acknowledged. K. Roberts and S. Duhachek are acknowledged for their help with fluorescence measurements. M.A. and R. P. acknowledge support from the DGI CYT (Grant PB 98-1632; Spain). Research at the National Renewable Energy Laboratory was sponsored by the Division of Energy Biosciences, U.S. Department of Energy. NREL is operated for USDOE by the Midwest Research Institute under Contract DE-AC36-98-GO10337.

References and Notes

(1) Bricker, T. M. *Photosynth. Res.* **1990**, *24*, 1.
(2) Rhee, K.-H.; Morris, E. P.; Barber, J.; Kühlbrandt, W. *Nature* **1998**, *396*, 283.
(3) Rhee, K.-H.; Morris, E. P.; Zheleva, D.; Hankamer, B.; Kühlbrandt, W.; Barber, J. *Nature* **1997**, *389*, 522.
(4) Delepelaire. P.; Chua, N.-H. *Proc. Natl. Acad. Sci. U.S.A.* **1979**, *76*, 111.
(5) Tang, X.-S.; Satoh, K. *Plant Cell Physiol.* **1984**, *25*, 935.
(6) De Vitry, C.; Wollen, F.-A.; Delepelaire, P. *Biochim. Biophys. Acta* **1984**, *767*, 415.
(7) Akabori, K.; Tsukamoto, H.; Tsukihara, J.; Nagatsuka, T.; Motokowa, O.; Toyoshima, Y. *Biochim. Biophys. Acta* **1988**, *932*, 345.

(8) Barbato, R.; Race, H. L.; Friso, G.; Barber, J. *FEBS Lett.* **1991**, *286*, 86.
(9) Alfonso, M.; Montoya, G.; Cases, R.; Rodríguez, R.; Picorel, R. *Biochemistry* **1994**, *33*, 10494.
(10) Zheleva, D.; Sharma, J.; Panico, M.; Morris, H. R.; Barber, J. *J. Biol. Chem.* **1998**, *273*, 16122.
(11) Hankamer, B.; Barber, J.; Boekema, E. J. *Annu. Rev. Plant Phys. Plant Mol. Biol.* **1997**, *48*, 641.
(12) Boekema; E. J.; Hankamer, B.; Bald, D.; Kruip, J.; Nield, J.; Boonstra, A. F.; Barber, J.; Rögner, M. *Proc. Natl. Acad. Sci. U.S.A.* **1995**, *92*, 175.
(13) Boekema, E. J.; van Room, H.; van Breemen, J. F. L.; Dekker: J. P. *Eur. J. Biochem.* **1999**, *266*, 444.
(14) Eijckelhoff, C.; Dekker, J. P.; Boekema, E. J. *Biochim. Biophys. Acta* **1997**, *1321*, 10.
(15) Mori, H.; Yamamoto, Y. *Biochim. Biophys. Acta* **1992**, *1100*, 293.
(16) Wang, J.; Shan, J.; Xu, Q.; Ruan, X.; Gong, Y.; Kuang, T.; Zhao, N. *J. Photochem. Photobiol. B: Biol.* **1999**, *50*, 189.
(17) Carbonera, D.; Giacometti, G.; Agostini, G.; Angerhofer, A.; Aust, V. *Chem. Phys. Lett.* **1992**, *194*, 275.
(18) Dekker, J.; Hassoldt, A.; Pettersson, Å.; van Room, H.; Groot, M.-L.; van Grondelle, R. In *Photosynthesis: From Light to Biosphere*; Mathias, P., Ed.; Kluwer Academic Publishers: Dordrecht, The Netherlands, 1995; Vol. 1, p 53.
(19) Alfonso, M.; Montoya, G.; Cases, R.; Rodríguez, R.; Picorel, R. *Biochemistry* **1994**, *33*, 10494.
(20) Breton, J.; Katoh, S. *Biochim. Biophys.* **1987**, *892*, 99.
(21) Rätsep, M.; Johnson, T. W.; Chitnis, P. R.; Small, G. J. *J. Phys. Chem. B* **2000**, *104*, 836.
(22) Pålsson, L.-O.; Flemming, C.; Gobets, B.; van Grondelle, R.; Dekker: J. P.; Schlodder, E. *Biophys. J.* **1998**, *74*, 2611.
(23) Chang, H.-C.; Jankowiak, R.; Yocum, C. F.; Picorel, R.; Alfonso, M.; Seibert, M.; Small, G. J. *J. Phys. Chem.* **1994**, *98*, 7717; *J. Phys. Chem.* **1994**, *98*, 7725.
(24) Groot, M.-L.; Frese, R. N.; Weerd, F. L.; Bromek, K.; Petterson, A.; Peterman, E. J. G.; van Stokkum, I. H. M.; van Grondelle, R.; Dekker, J. P. *Biophys. J.* **1999**, *77*, 3328.
(25) Jankowiak, R.; Tang, D.; Small, G. J.; Seibert, M. *J. Phys. Chem.* **1989**, *93*, 1649.
(26) Tang, D.; Jankowiak, R.; Seibert, M.; Small, G. J. *Photosynth. Res.* **1991**, *27*, 19.
(27) Chang, C.-H.; Jankowiak, R.; Reddy, N. R. S.; Small, G. J. *Chem. Phys.* **1995**, *197*, 307.
(28) Kim, W.-H.; Reinot, T.; Hayes, J. M.; Small, G. J. *J. Phys. Chem.* **1995**, *99*, 7300.
(29) Reinot, T.; Kim, W.-H.; Hayes, J. M.; Small, G. J. *J. Chem. Phys.* **1996**, *104*, 793.
(30) Rätsep, M.; Wu, H.-M.; Hayes, J. M.; Blankenship, R. E.; Cogdell, R. J.; Small, G. J. *J. Phys. Chem. B* **1998**, *102*, 4035.
(31) Rätsep, M.; Wu, H.-M.; Hayes, J. M.; Small, G. J. *Spectrochim. Acta A* **1998**, *54*, 1279.
(32) Small, G. J. *Chem. Phys.* (Special Issue) **1995**, *197*, 239.
(33) Pieper, J.; Rätsep, M.; Jankowiak, R.; Irrgang, K.-D.; Voigt, J.; Renger, G.; Small, G. J. *J. Phys. Chem. A* **1999**, *103*, 2412.
(34) Pieper, J.; Irrgang, K.-D.; Rätsep, M.; Voigt, J.; Renger, G.; Small, G. J. *Photochem. Photobiol*. **2000**, *71*, 574.
(35) Hayes, J. M.; Matsuzaki, S.; Rätsep, M.; Small, G. J. *J. Phys. Chem. B* **2000**, *104*, 5625.
(36) Shu, L.; Small, G. J. *J. Opt. Soc. Am. B* **1992**, *9*, 738.
(37) Jankowiak, R.; Hayes, J. M.; Small, G. J. *Chem. Rev.* **1993**, *93*, 1471.
(38) Middendorf, T. R.; Mazzola, L. T.; Lao, K.; Steffen, M. A.; Boxer, S. G. *Biochim. Biophys. Acta* **1993**, *1143*, 223.
(39) Kador, L.; Haarer, D.; Personov, R. *J. Chem. Phys.* **1987**, 86, 5300.
(40) Gafert, J.; Friedrich, J.; Vanderkooi, J. M.; Fidy, J. *J. Phys. Chem.* **1995**, *99*, 5233.
(41) Reddy, N. R. S.; Jankowiak, R.; Small, G. J. *J. Phys. Chem.* **1995**, *99*, 16168.
(42) Wu, H.-M.; Rätsep, M.; Jankowiak, R.; Cogdell, R. J.; Small, G. J. *J. Phys. Chem. B* **1997**, *101*, 7641.
(43) Wu, H.-M.; Rätsep, M.; Jankowiak, R.; Cogdell, R. J.; Small, G. J. *J. Phys. Chem. B* **1998**, *102*, 4023.
(44) Reddy, N. R. S.; Picorel, R.; Small, G. J. *J. Phys. Chem.* **1992**, *96*, 6458.
(45) den Hartog, F. T. H.; Dekker: J. P.; van Grondelle, R.; Völker, S. *J. Phys. Chem. B* **1998**, *102*, 11007.
(46) Jankowiak, R.; Rätsep, M.; Picorel, R.; Seibert, M.; Small, G. J. *J. Phys. Chem. B* **1999**, *103*, 9759.
(47) den Hartog, F. T. H.; Vacha, F.; Lock, A. J.; Barber, J.; Dekker: J.; Völker, S. *J. Phys. Chem. B* **1998**, *102*, 9174.
(48) Wu, H.-M.; Reddy, N. R. S.; Cogdell, R. J.; Muenke, C.; Michel, H.; Small, G. J. In *Proceedings of the HBRS '96 International Conference, Molecular Crystals and Liquid Crystals* **1996**, *291*, 163.
(49) Fetisova, Z. G.; Mauring, K. *FEBS Lett.* **1993**, *323*, 159.
(50) Psencik, J.; Polivka, T.; Nemec, P.; Dian, J.; Kudrna, J.; Maly, P.; Hala, J. *J. Phys. Chem. A* **1998**, *102*, 4392.
(51) Narasimhan, L. R.; Littau, K. A.; Pack, D. W.; Bai, Y. S.; Elschner, A.; Fayer, M. D. *Chem. Rev.* **1990**, *90*, 439.
(52) Völker, S. In *Relaxation Processes in Molecular Excited States*; Fünfschilling, J., Ed.; Kluwer Academic Publishers: Dordrecht, The Netherlands, 1989; p 113.
(53) Jankowiak, R.; Small, G. J. *Chem. Phys. Lett.* **1993**, *207*, 436.
(54) Rätsep, M.; Blankenship, R. E.; Small, G. J. *J. Phys. Chem. B* **1999**, *103*, 5736.
(55) Vasil'ev, S.; Irrgang, K.-D.; Schrötter, T.; Bergmann, A.; Eichler, H.-J.; Renger, G. *Biochemistry* **1997**, *36*, 7503.
(56) Matsuzaki, S.; Zazubovich, V.; Rätsep, M.; Hayes, J. M.; Small, G. J *J. Phys. Chem. B*, submitted.
(57) Pieper, J.; Irrgang, K.-D.; Rätsep, M.; Voigt, J.; Renger, G.; Small, G. J. *Photochem. Photobiol*. **2000**, *71*, 574.
(58) Hayes, J. M.; Gillie, J. K.; Tang, D.; Small, G. J. *Biochim. Biophys. Acta* **1988**, *932*, 287.